

## RED CELLS, IRON, AND ERYTHROPOIESIS

# Membrane skeleton modulates erythroid proteome remodeling and organelle clearance

Yijie Liu,<sup>1,2</sup> Yang Mei,<sup>1,2</sup> Xu Han,<sup>1,2</sup> Farida V. Korobova,<sup>3</sup> Miguel A. Prado,<sup>4</sup> Jing Yang,<sup>1,2</sup> Zhangli Peng,<sup>5</sup> Joao A. Paulo,<sup>4</sup> Steven P. Gygi,<sup>4</sup> Daniel Finley,<sup>4</sup> and Peng Ji<sup>1,2</sup>

<sup>1</sup>Department of Pathology, Feinberg School of Medicine, <sup>2</sup>Robert H. Lurie Comprehensive Cancer Center, and <sup>3</sup>Center for Advanced Microscopy, Northwestern University, Chicago, IL; <sup>4</sup>Department of Cell Biology, Harvard Medical School, Boston, MA; and <sup>5</sup>Department of Bioengineering, University of Illinois at Chicago, Chicago, IL

## KEY POINTS

- mDia2 is a master regulator of membrane skeleton integrity that modulates reticulocyte maturation.
- Chmp5 mediates the functions of mDia2 through the regulation of proteome remodeling and organelle clearance.

**The final stages of mammalian erythropoiesis involve enucleation, membrane and proteome remodeling, and organelle clearance. Concomitantly, the erythroid membrane skeleton establishes a unique pseudohexagonal spectrin meshwork that is connected to the membrane through junctional complexes. The mechanism and signaling pathways involved in the coordination of these processes are unclear. The results of our study revealed an unexpected role of the membrane skeleton in the modulation of proteome remodeling and organelle clearance during the final stages of erythropoiesis. We found that diaphanous-related formin mDia2 is a master regulator of the integrity of the membrane skeleton through polymerization of actin protofilament in the junctional complex. The mDia2-deficient terminal erythroid cell contained a disorganized and rigid membrane skeleton that was ineffective in detaching the extruded nucleus. In addition, the disrupted skeleton failed to activate the endosomal sorting complex required for transport-III (ESCRT-III) complex, which led to a global defect in proteome remodeling, endolysosomal trafficking, and autophagic organelle clearance. Chmp5, a component of the ESCRT-III complex, is regulated by mDia2-dependent activation of the serum**

**response factor and is essential for membrane remodeling and autophagosome-lysosome fusion. Mice with loss of Chmp5 in hematopoietic cells in vivo resembled the phenotypes in mDia2-knockout mice. Furthermore, overexpression of Chmp5 in mDia2-deficient hematopoietic stem and progenitor cells significantly restored terminal erythropoiesis in vivo. These findings reveal a formin-regulated signaling pathway that connects the membrane skeleton to proteome remodeling, enucleation, and organelle clearance during terminal erythropoiesis. (*Blood*. 2021;137(3):398-409)**

## Introduction

Reticulocytes formed after enucleation of the orthochromatic erythroblasts contain organelles and nonhemoglobin proteins that are largely eliminated during maturation. Maturation of reticulocytes is divided into 2 stages. The early-stage reticulocytes (R1), immediately after the extrusion of nuclei, are motile, irregular, and large. The more mature R2 stage reticulocytes are nonmotile and clear of organelles. Through R1 and R2, membrane transferrin receptor, adhesion molecules, and many other cytoplasmic proteins are depleted to establish a hemoglobin-predominant proteome.<sup>1,2</sup> Reticulocytes also undergo volume reduction that involves membrane loss and exocytosis.<sup>3</sup> In addition, the reticulocyte membrane skeleton is remodeled to establish the biconcave and stable erythrocyte structure.<sup>4-8</sup> Knowledge accumulated in the past few decades reveals several processes in protein removal and organelle clearance during reticulocyte maturation, in which multivesicular body formation, autophagy, and exocytosis are involved.<sup>1,9</sup> However, the mechanisms of these processes remain elusive. It is particularly unclear whether and how the membrane skeleton coordinates

with proteome remodeling and organelle clearance during terminal erythropoiesis.

mDia2 is a diaphanous-related formin protein involved in linear actin polymerization and is highly upregulated in the late stages of terminal erythropoiesis.<sup>10,11</sup> mDia2 contains formin homology-1 and -2 domains that are important for actin polymerization. The N terminus of the mDia2 protein contains a Rho GTPase binding domain, a diaphanous-inhibitory domain, and a dimerization domain. On the C terminus, there is a diaphanous auto-regulatory domain (DAD) that binds to the diaphanous-inhibitory domain to form an auto-inhibitory loop when mDia2 is inactivated.<sup>11-13</sup> Mutations in the DAD domain or N-terminal regions disrupt this autoinhibitory structure and lead to the constitutive activation of mDia formin proteins.<sup>14-17</sup> In addition, binding of Rho GTPase to the GTPase binding domain relieves the autoinhibitory loop, to activate mDia formins under physiologic conditions.<sup>11</sup>

mDia formins are reported to be involved in a variety of cellular processes.<sup>11,18</sup> Mouse genetic studies by us and others showed

embryonic lethality in mDia2-knockout mice, with major defects in the hematopoietic system.<sup>19,20</sup> Loss of mDia2 influences terminal erythropoiesis at different stages, which manifests as compromised cytokinesis and enucleation. In this respect, the mDia2 conditional and hematopoietic-specific knockout mouse model provides a valuable tool for studying terminal erythropoiesis in vivo in adults, which is not possible to perform using whole-body knockout mice. With this model, we showed that mDia2 is indispensable for the motility of R1 reticulocytes, membrane skeleton integrity, and clearance of unnecessary proteins and organelles in maturing reticulocytes. We also revealed a novel mDia2-Chmp5 pathway and mDia2-regulated endosomal sorting complex required for transport-III (ESCRT III) complex in reticulocyte maturation. The results of these experiments underline the critical roles of the integrity of the membrane skeleton in the modulation of erythroid proteome remodeling and organelle clearance.

## Methods

### Mice

Genetically modified, tissue-specific mDia2-knockout mice on a C57/BL6 background have been described.<sup>20,21</sup> Congenic mice carrying CD45.1 antigen were purchased from Charles River (B6-LY-5.2/Cr, strain code: 564). C57/BL6 wild-type, CAG-Cas9 transgenic (026179), and Vav-Cre (008610) mice were purchased from Jackson Laboratory. GFP-LC3 mice were kindly provided by Congcong He (Northwestern University, Chicago, IL). GFP-LC3 transgenic mice were crossed with mDia2<sup>fl/fl</sup> Vav-Cre mice to obtain mDia2<sup>fl/fl</sup> GFP-LC3 and mDia2<sup>fl/fl</sup> Vav-Cre GFP-LC3 mice. All experiments involving animals were conducted in accordance with the Guide for the Care and Use of Laboratory Animals and were approved by the Institutional Animal Care and Use Committee at Northwestern University.

### In vitro culture of erythroid cells

Purification and in vitro culture of mouse bone marrow lineage-negative cells into cells of the erythroid lineage were performed as previously described.<sup>10</sup> In brief, lineage-negative cells were purified with a mouse lineage antibody cocktail (559971; BD Biosciences) and cultured in erythropoietin-containing medium for 48 hours. By day 2, ~20% to 30% of the cells were enucleated. The cells were harvested at various time points, as indicated in the different experiments, for further characterization.

### Expression constructs

The MSCV-IRES-hCD4 (MICD4) construct has been described.<sup>10</sup> The pCINeo-mChmp5 construct was purchased from Addgene (11771), mChmp5 was polymerase chain reaction (PCR) amplified and subcloned into the MICD4 vector through the EcoRI and NotI sites. The MICD4-SRF construct was described previously.<sup>22</sup> The expression construct carrying an HA-tagged, constitutively active form of human serum response factor (SRF) was kindly provided by Naren Ramanan (Indian Institute of Science, Bangalore, India) and was PCR amplified and subcloned into the MICD4 vector. pGL4-Chmp5 promoter fragments were subcloned into the pGL4.24(luc2P/minP) vector (E842A; Promega) between the HindIII and XhoI sites. The autophagy reporter construct pCDH-puro-mCherry-EGFP-LC3 was kindly provided by Congcong He.

### STORM imaging

The stochastic optical reconstruction microscopy (STORM) imaging analysis was performed as previously described.<sup>23</sup>

### Scanning electron microscopy

Erythroblasts and reticulocytes were cultured as described. The cells were collected or sorted, and washed 3 times with phosphate-buffered saline, followed by fixation in 2% glutaraldehyde (Polysciences) in 100 mM phosphate buffer (pH 7.2) overnight at 4°C. The cells were then processed and examined with a JEOL NeoScope scanning electron microscope.

### Transmission electron microscopy and immunogold staining

In vitro cultured erythroblasts and reticulocytes were collected and washed 3 times with phosphate-buffered saline, followed by fixation in 2% glutaraldehyde (Polysciences) and 100 mM phosphate buffer (pH 7.2) overnight at 4°C. For red blood cell (RBC) membrane skeleton transmission electron microscopy (TEM), ghost RBCs were prepared by incubation of RBCs in a hypotonic buffer (0.5 mM phosphate and 0.1 mM EDTA [pH 7.4]) for 15 minutes and mounted on cover slides. Immunogold staining was used to detect mDia2 localization on the RBC membrane skeleton, as previously described.<sup>24</sup> The human mDia2 antibody (14342-1-AP; Proteintech) had been validated.<sup>25,26</sup> The cells were processed and examined with an FEI Tecnai Spirit G2 transmission electron microscope.

### Live imaging of reticulocyte motility

Erythroblasts purified from the bone marrow were cultured in erythropoietin-containing medium for 48 hours. A fluorescent nuclear-staining dye was added to the culture medium (R37106; ThermoFisher) at 37°C for 15 minutes. Movies were taken with a Nikon W1 Dual Cam Spinning Disk Confocal Microscope (objective lens: Apo TIRF 60×/1.49 oil). The data were analyzed with NIS software and ImageJ.

### RBC ghost preparation

RBC ghost preparation was performed according to a published method.<sup>27</sup>

### Bone marrow transplantation

The bone marrow transplantation was performed as previously described.<sup>21,28-30</sup>

### Immunofluorescence analysis

Immunofluorescence analysis was performed as previously described.<sup>29,31</sup> Primary antibodies were Chmp5 (sc-374338; Santa Cruz Biotechnology), LAMP1 (L1418; Sigma), LBPA (MABT837; Sigma), M6PR (ab2733; Abcam), lysosome tracker green (L7526; ThermoFisher), mitochondrial tracker deep red (MitoTracker M22426; Invitrogen), and LC3B (ab48394; Abcam). Immunofluorescence images were obtained with an Olympus IX70 Inverted Fluorescence Microscope (objective lens: U-PLAN S-APO 1003 oil, 1.4 numeric aperture, 0.12-mm working distance; differential interference contrast) and a Nikon X1 Spinning Disk confocal microscope (objective lens: Apo TIRF 100×/1.49 oil immersion). The images were analyzed with NIS Elements software and ImageJ.

### Flow cytometry

Flow cytometry of differentiation and enucleation of cultured mouse bone marrow erythroblasts were performed as previously described.<sup>10,31-34</sup>

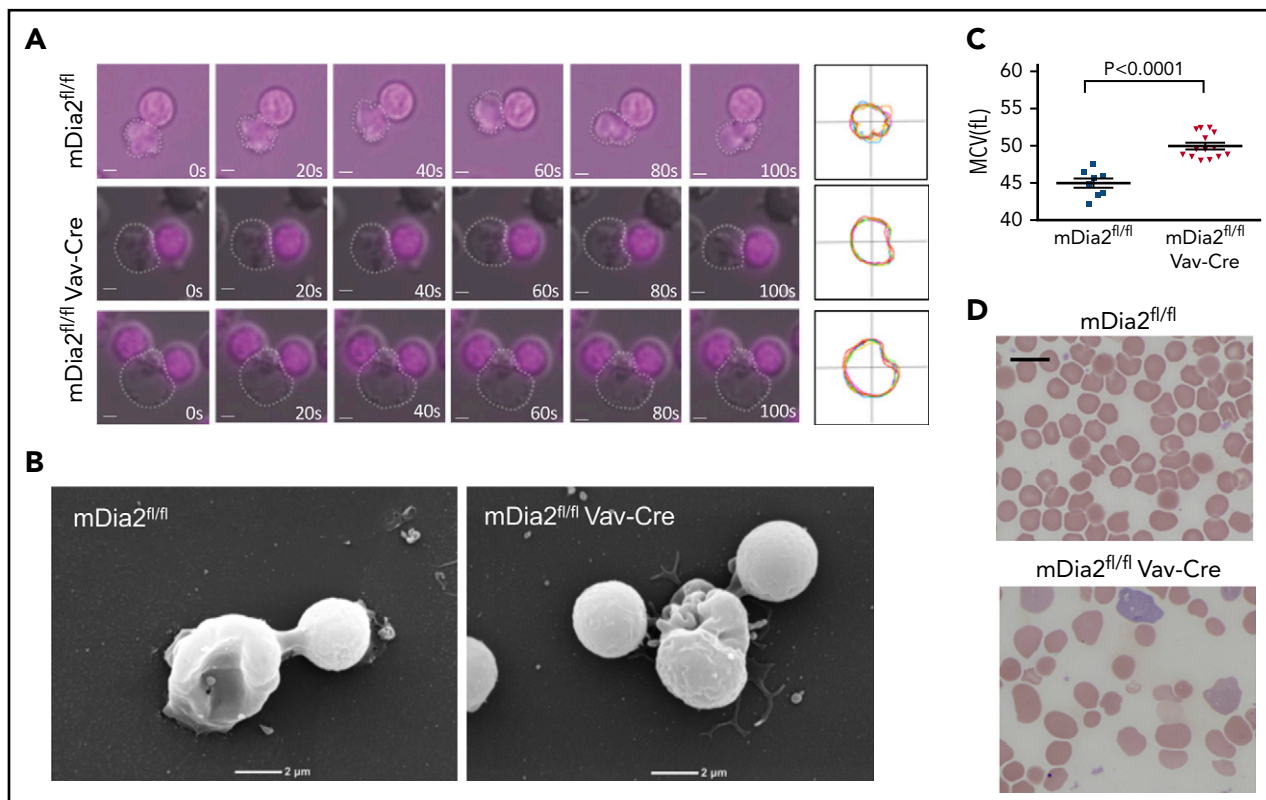


**Figure 1. mDia2 is essential for the mobility of R1 reticulocytes.** (A) Time lapse real-time microscopy of enucleating erythroid cells derived from cultured bone marrow erythroblasts obtained from the indicated mice. Still frames of cells at the indicated times (seconds) are shown. The bottom panels show an enucleating cell with 2 extruding nuclei. Nuclei were stained with NucRed Live 647. Bars represent 1  $\mu$ m. White dots outline R1 reticulocytes. Far right panels show the overlapped outlines of the dynamic reticulocytes at different time points. (B) Scanning electron microscopy analyses of enucleating cells from panel A. (C) Mean corpuscular volume of RBCs from peripheral blood of the indicated mice at 1 month of age. (D) Wright-Giemsa-stained peripheral blood smears from the indicated mice at 1 month of age. Bar represents 10  $\mu$ m.

## Chloroquine treatment

Chloroquine (CQ) was purchased from Sigma (C6628-25G). Bone marrow lineage-negative cells were purified and cultured for 48 hours. CQ was then added to the cell medium to a final concentration of 100  $\mu$ M and incubated for an additional 2 hours. Cells were collected and fixed for further analyses.

## Retroviral shRNA design

A retroviral short hairpin RNA (shRNA) oligo against mChmp5 was designed with an online shRNA designer (<http://simu.wi.mit.edu>). The shRNA oligos were cloned into the MSCV-U3-H1 retroviral vector, as previously described.<sup>10</sup>

## Statistics

Results are expressed as the mean  $\pm$  SEM, unless otherwise indicated. Statistical comparisons between 2 groups were performed with a 2-tailed unpaired Student t test, with GraphPad Prism version 6.0 software.

## Results

### mDia2 is essential for the integrity of the membrane skeleton

We have shown that hematopoietic-specific, mDia2-deficient mice exhibit anemia and ineffective erythropoiesis.<sup>20</sup> To determine the role of mDia2 in reticulocyte maturation, we analyzed bone marrow reticulocytes from the mice by using live imaging. Knockout of

mDia2 was first confirmed by the loss of mDia2 expression with hematopoietic-specific Cre expression (supplemental Figure 1A-B, available on the *Blood* Web site). We found that R1 reticulocytes from mDia2-deficient mice were rigid and showed little motility during enucleation compared with their wild-type counterparts (Figure 1A; supplemental Movies 1 and 2). Work by us and others has demonstrated that mDia2 is critical for terminal erythropoiesis and enucleation.<sup>10,19,20</sup> Loss of mDia2 compromises cytokinesis and leads to a significant increase in binucleated orthochromatic erythroblasts, which are precursor cells in the last stage of terminal erythropoiesis before enucleation. Interestingly, we also found enucleating cells with 2 nuclei attached to the rigid reticulocyte (Figure 1A-B; supplemental Movie 3), indicating that orthochromatic erythroblasts with dysplastic nuclei can still enucleate.

We have reported that Rac GTPases are upstream regulators of mDia2. Brief Rac inhibitor treatment of the cultured mouse erythroblasts immediately before enucleation significantly inhibits enucleation.<sup>10</sup> To investigate whether Rac GTPases are also involved in reticulocyte motility, we treated mouse bone marrow erythroblasts for 5 minutes at 35 hours in culture, when the cells started to enucleate, and analyzed the motility of the R1 reticulocytes in real time. Indeed, this brief treatment phenocopied the motility defects of mDia2-deficient reticulocytes (supplemental Figure 1C). Overall, these results demonstrate that mDia2 is involved in the motility of R1 reticulocytes that is critical for the detachment of the extruded nuclei in the last step of enucleation.<sup>35</sup>

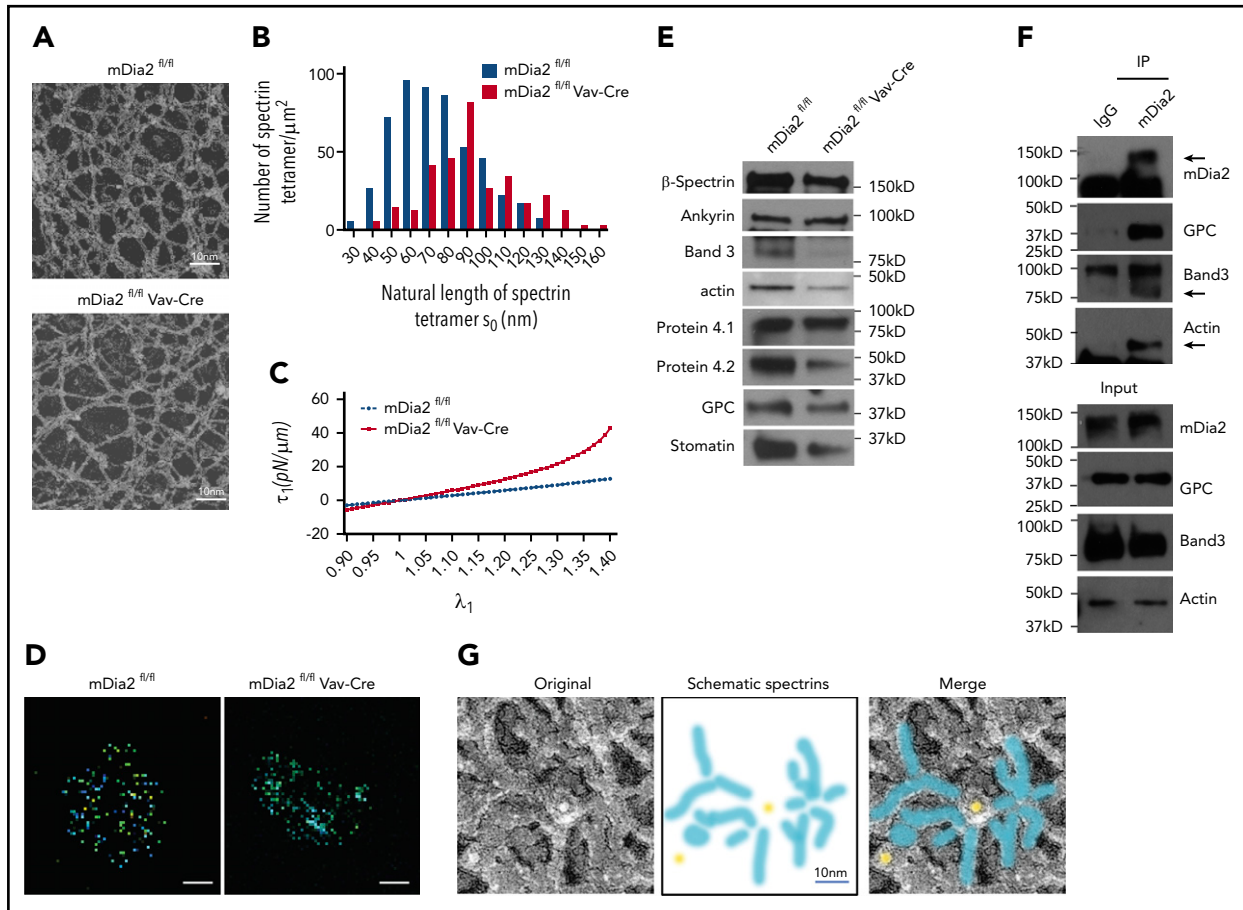


**Figure 2. Loss of mDia2 compromises erythrocyte membrane skeleton structure.** (A) TEM study of the membrane skeleton of ghost erythrocytes from the indicated mice. Data are representative of 13 randomly selected fields. (B) The length distributions of the spectrin tetramers with corresponding frequencies in ghost erythrocytes calculated based on the TEM images in panel A. (C) Computationally predicted stress of the membrane skeleton under uniaxial tension with the increased deformation ( $\lambda_1$ ) of the indicated mice. A shear modulus  $\mu_0 = 13.1$  pN/ $\mu\text{m}$  is estimated for mDia2<sup>fl/fl</sup> cells and  $\mu_0 = 26.5$  pN/ $\mu\text{m}$  for mDia2<sup>fl/fl</sup>Vav-Cre cells. (D) STORM imaging analyses of actin protofilaments in ghost erythrocytes from the indicated mice. Bars represent 1  $\mu\text{m}$ . (E) Western blot analyses of the indicated erythroid membrane skeleton proteins of ghost erythrocytes from the indicated mice. An equal number of cells was used. (F) Immunoprecipitation assay using IgG or mDia2 antibodies in normal human ghost erythrocytes. Western blot analyses were performed to determine the coprecipitated proteins. (G) Immunogold stain of mDia2 and electron microscopy analysis of normal human ghost erythrocytes. Yellow dots and blue stripes in the schematic spectrin graph indicate gold particles and spectrin bands, respectively.

The defects in the motility of R1 reticulocytes prompted us to analyze the membrane skeleton of the erythrocytes in mDia2<sup>fl/fl</sup>Vav-Cre mice. RBCs in mDia2-deficient mice showed macrocytosis (Figure 1C) and anisopoikilocytosis, with numerous irregularly shaped erythrocytes (Figure 1D).<sup>20</sup> Through TEM of hemoglobin-depleted ghost RBCs, we found that mDia2-deficient cells showed significantly elongated spectrin chains (Figure 2A), which indicates reduced flexibility of the pseudo-hexagonal erythroid membrane skeleton meshwork. The median calculated length distribution of spectrin tetramer in the erythrocytes of mDia2<sup>fl/fl</sup>Vav-Cre mice was shifted significantly to the right (ie, longer spectrin length), compared with that of the control (Figure 2B). This shift led to an enhanced increase in membrane skeleton stress, with membranes stretched under uniaxial tension (Figure 2C). The extended spectrin chains were also compatible with macrocytosis and suggested a failure of volume reduction in the maturing reticulocytes. Consistent with the role of mDia2 in actin polymerization, STORM imaging analysis showed that the short actin protofilaments were irregularly distributed in mDia2-deficient erythrocytes (Figure 2D). Western blot analyses on ghost erythrocytes further revealed that many membrane skeleton proteins were significantly decreased in mDia2-deficient erythrocytes (Figure 2E). These results demonstrate a

critical role of mDia2 in maintaining the integrity of the erythroid membrane skeleton. To determine the localization of mDia2 on the skeleton, we performed a coimmunoprecipitation assay in ghost erythrocytes from normal human RBCs. The result showed that mDia2 bound to band 3, actin, and glycophorin C, which are protein components of the junctional complex that are critical in the maintenance of the pseudo-hexagonal meshwork in the erythroid membrane skeleton (Figure 2F). We further performed immunogold labeling of mDia2 in normal human erythrocytes, followed by electron microscopy, which also showed localization of mDia2 at the junctional complex (Figure 2G).

### Loss of mDia2 leads to impaired membrane and proteome remodeling and organelle clearance

Given the significance of mDia2 in the integrity of the membrane skeleton, we next investigated whether it is also involved in membrane remodeling and organelle clearance during reticulocyte maturation. We first analyzed several proteins, such as CD71 and CD44, that are programmed to be downregulated during the late stages of terminal erythropoiesis.<sup>36-38</sup> Indeed, the surface levels of CD71 and CD44 were significantly increased in mDia2-deficient reticulocytes compared with levels on the

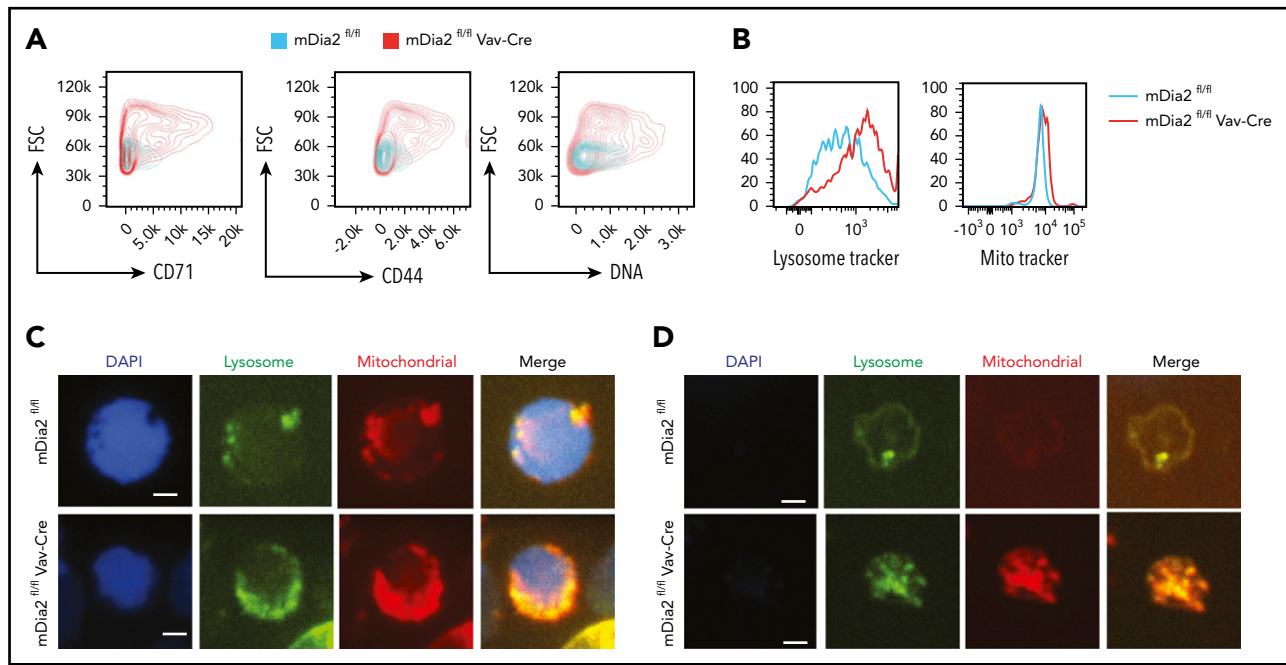


**Figure 3. mDia2 is involved in membrane remodeling and organelle clearance during terminal erythropoiesis.** (A) Lineage-negative cells from the bone marrow of the indicated mice were cultured in erythropoietin-containing medium for 2 days. Flow cytometric analysis was performed to determine the surface levels of the indicated proteins, DNA, and forward scatter (FSC) in wild-type and mDia2-deficient reticulocytes. (B) Same as panel A except the cells were also stained with lysosome tracker and MitoTracker Red for the detection of lysosome and mitochondria content, respectively. (C-D) Fluorescence analyses of the indicated organelles in the orthochromatic stages of the erythroblasts (C) and reticulocytes (D) in the cells from panel B.

wild-type control cells (Figure 3A). This defect in the down-regulation of surface proteins in mDia2-deficient erythroid cells was also readily detected in the orthochromatic stage of terminal erythropoiesis (supplemental Figure 2A). The same phenotypes were observed in another mDia2 hematopoietic-specific knockout model in which mDia2 depletion was induced in adults (supplemental Figure 2B-C). mDia2-deficient reticulocytes were also much larger (forward scatter) than their wild-type counterparts. Although some managed to enucleate, mDia2-deficient reticulocytes contained a higher content of residual DNA than the controls (Figure 3A; supplemental Figure 2B). These data indicate that although the levels of many structural proteins were reduced in mDia2-deficient erythrocytes (Figure 2E), those that were programmed to be removed from the membrane failed to disappear. To further determine whether loss of mDia2 affects organelle clearance, we stained lysosomes and mitochondria in reticulocytes sorted from the cultured erythroblasts and indeed found increased levels with loss of mDia2 (Figure 3B-D).

Consistent with the flow cytometry and immunofluorescence assays, TEM analyses revealed significantly enlarged mDia2-deficient reticulocytes, with numerous organelles that failed to be cleared. Large multivesicular bodies (MVBs) that were uncommon in wild-type reticulocytes were also frequently observed in mDia2-deficient ones (Figure 4A, inset III). Accordingly, extracellular vesicles that are normally released through MVB fusion with the membrane were significantly reduced in the medium cultured with mDia2-deficient erythroid cells (Figure 4B). Furthermore, autophagic vacuoles, many resembling autophagosomes with double membranes, were also readily detected in mDia2-deficient orthochromatic erythroblasts (Figure 4C).

We next compared the proteome of mDia2-deficient and wild-type reticulocytes by using tandem mass tagging mass spectrometry in hemoglobin-depleted ghost reticulocytes. As expected, many membrane and skeleton proteins were decreased in mDia2-deficient cells. On the other hand, many nucleus- and chromosome-associated proteins were elevated (Figure 4D; supplemental Figure 3A-B; supplementary Data 1). A study revealed that UBE2O remodels the proteome of reticulocytes through ubiquitination and proteasome degradation of many substrates, predominantly ribosome proteins.<sup>39</sup> Our data demonstrate that mDia2 is involved in the clearance of other substrates, mainly DNA-associated proteins that are known to be cleared after extrusion of the nucleus during reticulocyte maturation.<sup>40</sup> This is also consistent with the increased DNA levels in mDia2-deficient reticulocytes (Figure 3A).

### Chmp5 is regulated by mDia2 and mediates the function of mDia2 during reticulocyte maturation

Defects in the detachment of the extruded nuclei in mDia2-deficient reticulocytes could also be related to compromised cytokinesis, which is supported by the increased binucleated orthochromatic erythroblasts that failed cytokinetic abscission in mDia2<sup>fl/fl</sup>Vav-Cre mice.<sup>20</sup> Cytokinesis involves the constriction of an actomyosin ring formation of microtubule arrays, and final abscission mediated by ESCRT proteins, which are known to be critical for various membrane remodeling activities, including endocytosis and subsequent degradation in the lysosomes. In this process, ESCRT-0, -I, and -II complexes are involved in the recognition of ubiquitinated cargo and inclusion in MVBs. The ESCRT-III complex is critical as multifunctional machinery for the invagination of vesicles to form MVBs, abscission of the vesicles, and regulation of late endosome function that induces lysosome degradation.<sup>41-47</sup> Given the defects in cytokinetic abscission and

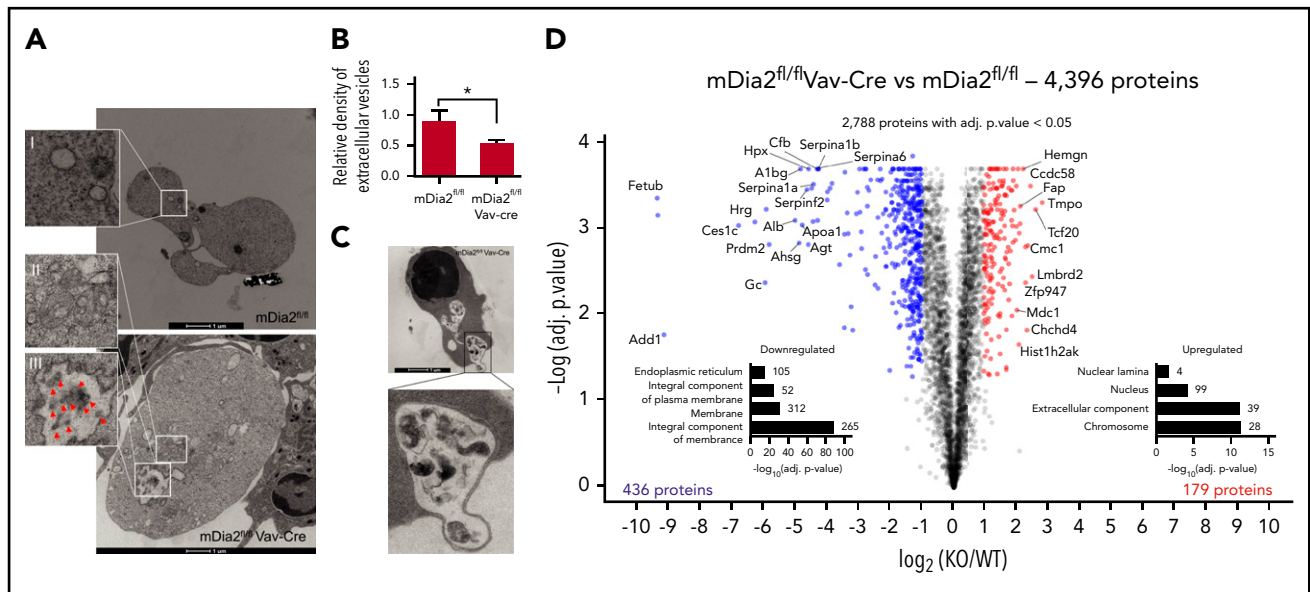


**Figure 4. Defect in endolysosomal and autolysosomal formation and proteome remodeling in mDia2-deficient erythroid cells.** (A) TEM studies of reticulocytes from mDia2<sup>fl/fl</sup>Vav-Cre mice (bottom) and mDia2<sup>fl/fl</sup> mice (top). An adjacent orthochromatic erythroblast (bottom right) with numerous organelles and vesicles is also seen. Bars represent 1  $\mu$ m. Arrows in inset III indicate vesicles. Insets II and III show increased organelles compared to inset I. (B) Lineage-negative cells from the bone marrow of the indicated mice were cultured in erythropoietin-containing medium for 2 days. Quantitative analyses were performed of extracellular vesicles from the culture medium. \* $P < .05$ . (C) TEM analysis of a representative orthochromatic stage erythroblast from mDia2<sup>fl/fl</sup>Vav-Cre mice. Images are representative of 10 randomly selected fields. (D) Volcano plot of a quantitative proteomic study. Proteins significantly upregulated (red) or downregulated (blue) in mDia2-deficient reticulocytes are shown. Kyoto Encyclopedia of Genes and Genomes pathway enrichment analyses of proteins upregulated or downregulated by >25% are shown. The number of proteins per group is indicated on the right. The experiments were repeated 3 times, and the data were obtained with combined individual analyses.

increased MVBs in the late stages of terminal erythropoiesis, we reasoned that the ESCRT-III complex could be important in mediating the functions of mDia2, including membrane and proteome remodeling and organelle clearance. To test this hypothesis, we first analyzed the expression of the components of ESCRT-III complex in the late stage of terminal erythropoiesis in mDia2<sup>fl/fl</sup>Vav-Cre mice and wild-type controls. Indeed, the mRNA levels of many genes encoding various ESCRT-III components were significantly downregulated in mDia2-deficient erythroblasts (supplemental Figure 4A-B).

Among these downregulated ESCRT-III components, Chmp5 is unique in that it is not necessary for MVB formation, as are other proteins in the complex. Instead, it is critical for the maturation of MVBs into lysosomes.<sup>48,49</sup> The reported phenotypes of Chmp5-deficient cells, including the enlarged late endosomes/MVBs and upregulation of surface receptors,<sup>48</sup> resemble what we observed in mDia2-deficient terminal erythroid cells. Indeed, we found increased colocalization of LBPA and LAMP1 (endosome/MVB markers) in mDia2-deficient orthochromatic erythroblasts and reticulocytes (Figure 5A; supplemental Figure 4C), demonstrating a compromised maturation of MVBs to lysosomes. The expression level of Chmp5 remains constant across different stages of terminal erythropoiesis (supplemental Figure 4D-E). To study the relationship between mDia2 and Chmp5, we first confirmed the downregulation of Chmp5 protein, as well as several other components of the ESCRT-III complex, in the late stage of bone marrow terminal erythropoiesis in mDia2<sup>fl/fl</sup>Vav-Cre mice (supplemental Figure 4F). Immunofluorescence analysis showed Chmp5 localization between the dividing erythroblasts in cultured bone marrow erythroid cells from wild-type mice. In comparison, Chmp5 was barely detectable in the binucleated erythroblasts frequently found in mDia2-deficient mice (Figure 5B).

mDia2 formin proteins function not only in cell migration and adhesion through their direct roles in linear actin polymerization, but also in transcriptional regulation through activation of the megakaryocytic acute leukemia (MAL)-SRF pathway.<sup>11,50,51</sup> By promoting actin polymerization, mDia2 formins release G-actin monomers from MAL protein. The released MAL translocates into the nucleus, where it dimerizes with SRF to drive SRF-dependent gene expression of many cytoskeleton-related genes.<sup>52,53</sup> Given the reduced expression of Chmp5 in mDia2-deficient cells, we next determined whether Chmp5 is a direct transcriptional target of SRF. To this end, we performed an analysis to identify SRF responsive elements (SREs), the "CArG" box, on the promoter region of Chmp5, by using a transcription factor online binding site prediction tool,<sup>54</sup> and found 2 putative SREs in the Chmp5 promoter (Figure 5C). We then cloned these 2 SREs and inserted them individually ahead of the luciferase gene. SRE site 1, but not site 2, induced strong luciferase activity that was inhibited by the mutation that disrupted the SRE (Figure 5C). To confirm the binding of SRF to this site, we performed a chromatin immunoprecipitation (ChIP) assay and indeed revealed specific binding of SRF to the SRE on Chmp5 (Figure 5D). Consistent with the role of mDia2 in the regulation of SRF, loss of mDia2 significantly reduced the binding of SRF to the SRE on Chmp5 (Figure 5E). To further confirm the mDia2-SRF axis in the regulation of Chmp5 expression, we overexpressed SRF and transduced it into mDia2-deficient erythroblasts. As expected, the expression of Chmp5 was largely rescued by SRF (Figure 5F). Functionally, knockdown of Chmp5 in vitro through shRNA in wild-type bone marrow lineage-negative cells led to a significantly increased number of binucleated orthochromatic erythroblasts (Figure 5G-H). Knockout of Chmp5 in vitro and hematopoietic-specific knockout of Chmp5 in vivo through CRISPR-Cas9 also resulted in significantly increased binucleated orthochromatic

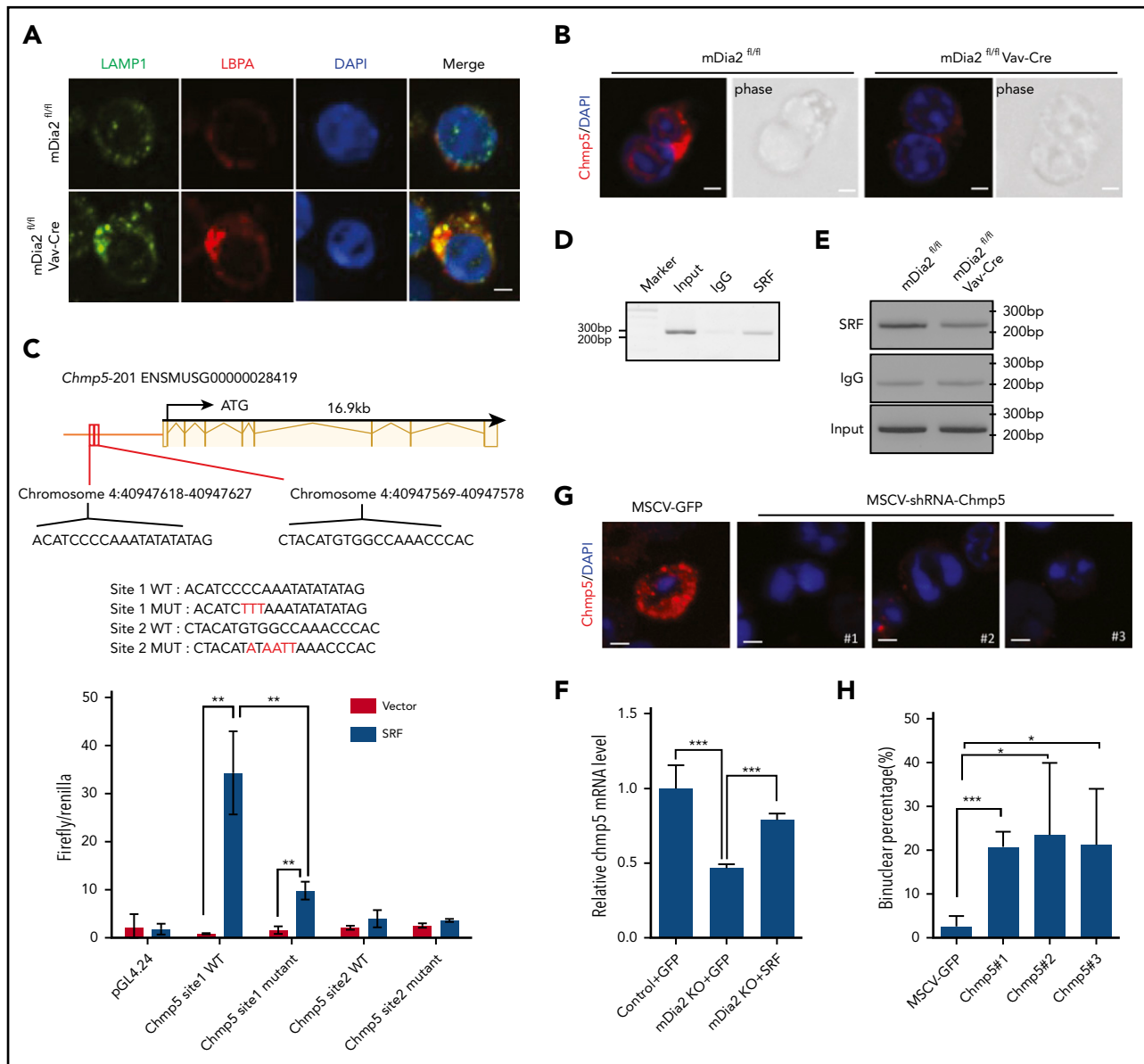


**Figure 5. ESCRT-III complex mediates the function of mDia2.** (A) Bone marrow lineage-negative cells from the indicated mice were cultured in erythropoietin-containing medium for 2 days. Immunofluorescent staining of the indicated markers on the orthochromatic erythroblasts was performed on day 2. Bar represents 1  $\mu$ m. Images are representative of 10 randomly selected fields. (B) Immunofluorescent staining of Chmp5 in the dividing cells of cultured erythroblasts from control and mDia2-deficient mice. Bars represent 1  $\mu$ m. Images are representative of 10 randomly selected fields. (C) View of the genomic region of Chmp5 with 2 predicated SREs in its promoter region. The sequences of these SREs and their mutant forms used in the luciferase assay are listed. The bottom panel is the luciferase reporter assay. 293T cells were cotransfected with luciferase reporters containing the indicated wild-type (WT) or mutant SREs (MUT), together with SRF-expressing constructs in the presence of a *Renilla* luciferase expression vector (pRL-TK). Firefly and *Renilla* luciferase activities were measured after 24 hours. \*\* $P < .01$ . (D) ChIP assay of day 2 cultured wild-type erythroblasts with the indicated antibodies followed by PCR of the SREs on the Chmp5 promoter. (E) ChIP assays as in panel D, using an SRF antibody or IgG on day 2 cultured erythroblasts from the indicated mice followed by PCR of the SREs on the Chmp5 promoter. (F) Real time reverse transcription–PCR analyses of Chmp5 mRNA levels of day 2 cultured erythroblasts from control or mDia2<sup>fl/fl</sup>Vav-Cre (knockout) mice transduced with the indicated genes on day 0. \*\*\* $P < .001$ . (G) Wild-type bone marrow lineage-negative cells were transduced with murine stem cell virus (MSCV) retroviruses expressing GFP and different shRNAs targeting Chmp5. The transduction efficiency was ~40% across all the constructs (not shown). The cells were then cultured for 2 days in erythropoietin-containing medium. Immunofluorescent stains of Chmp5 were performed. Images are representative of 5 randomly selected fields. Bars represent 1  $\mu$ m. (H) Quantification of binucleated orthochromatic erythroblasts in panel G. \* $P < .05$ ; \*\*\* $P < .001$ .

erythroblasts, organelle retention, and defects in membrane remodeling (supplemental Figure 5A–H).

### The mDia2-Chmp5 pathway is critical for fusion of autophagosomes and lysosomes

The ESCRT-III complex is reported to play a role in the fusion of autophagosomes to lysosomes.<sup>55</sup> The presence of increased autophagosomes in mDia2-deficient terminal erythroid cells

indicates a defect in autolysosome formation. We first analyzed the levels of autophagic flux in the late stages of terminal erythropoiesis through immunofluorescence stain and western blot analysis of LC3, which was dramatically increased in mDia2-deficient terminal erythroid cells (Figure 6A–B). In addition, we crossed mDia2-deficient mice with GFP-LC3 mice and obtained mDia2<sup>fl/fl</sup>/GFP-LC3 and mDia2<sup>fl/fl</sup>Vav-Cre/GFP-LC3 mice. The late-stage erythroblasts purified from the bone marrow of these mice indeed demonstrated

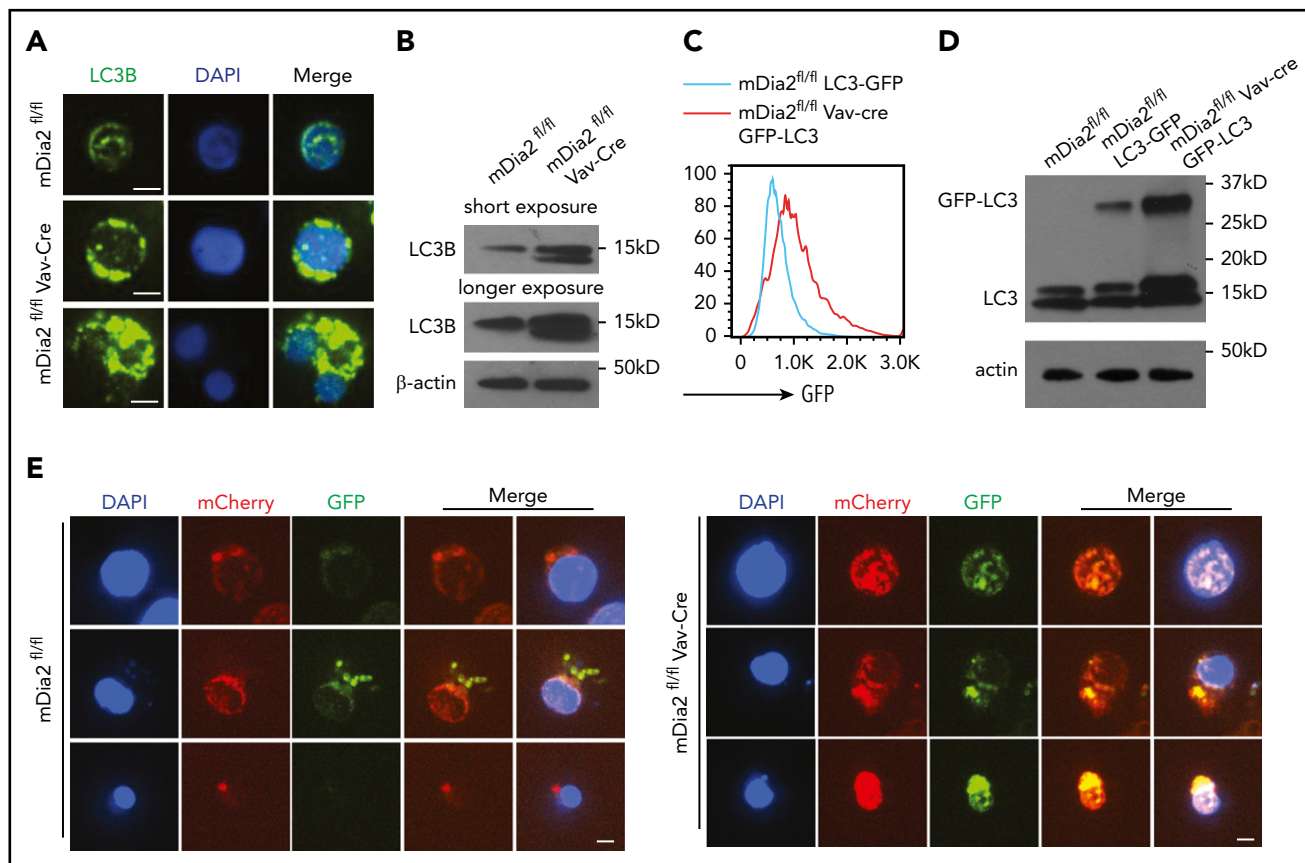


**Figure 6. Defects of autophagosome-lysosome fusion in mDia2-deficient erythroid cells.** (A) Lineage-negative cells from the bone marrow of the indicated mice were cultured in erythropoietin-containing medium for 2 days. Representative images of LC3B-stained orthochromatic erythroblasts are shown. Bars represent 2  $\mu$ m. Images are representative of 10 randomly selected fields. The bottom panels illustrate a binucleated orthochromatic erythroblast. (B) Western blot analysis of the cells in panel A. (C) Lineage-negative cells from the bone marrow of the indicated mice were cultured in erythropoietin-containing medium for 2 days. Flow cytometric analysis was performed to determine GFP intensity on the Ter119<sup>+</sup> DNA<sup>+</sup> erythroblasts. (D) Western blot analysis of the cells in panel C for the detection of GFP-LC3 and LC3. (E) Lineage-negative cells from the indicated mice were transduced with Lenti-mCherry-EGFP-LC3. The cells were cultured in erythropoietin-containing medium for 2 days. Representative images of erythroblasts at different developmental stages based on the nuclear size were presented. Bars represent 10  $\mu$ m. Images are representative of 10 randomly selected fields.

significantly increased GFP signals in cells from mDia2<sup>fl/fl</sup>Vav-Cre/GFP-LC3 mice (Figure 6C-D). To directly determine whether the fusion of autophagosomes with lysosomes is compromised, we transduced primary bone marrow erythroid progenitors with a tandem fluorescence-tagged LC3 (mCherry-EGFP-LC3). EGFP is sensitive to the acidic environment of lysosomes, whereas mCherry is more stable. An increase in the merged yellow signal suggests a defect in fusion with the lysosomes.<sup>56</sup> We analyzed the transduced erythroblasts after their maturation, as measured by progressive nuclear condensation. Compared with the control, mDia2-deficient erythroblasts showed markedly increased yellow signals across the differentiation stages (Figure 6E). Chloroquine is known to block autophagosome-lysosome fusion.<sup>57</sup> Treatment of mDia2-deficient erythroblasts with chloroquine induced no further increase in LC3 signal, which supports the defect in autophagosome-lysosome fusion with loss of mDia2 (supplemental Figure 6A). As expected, knockout of Chmp5 through sgRNA significantly induced autophagic flux (supplemental Figure 6B).

### Overexpression of Chmp5 ameliorates the defects in terminal erythropoiesis in mDia2-deficient mice

Our results strongly suggest that Chmp5 acts as a downstream effector of the mDia2-SRF axis in regulating ESCRT-III complex-mediated cytokinesis and global clearance of proteins and organelles

during the late stages of terminal erythropoiesis. To further demonstrate this, we first purified lineage-negative hematopoietic stem and progenitor cells from the bone marrow of mDia2<sup>fl/fl</sup>Vav-Cre mice and infected them with retroviruses expressing a constitutively active mDia2 mutant,  $\Delta$ DAD (supplemental Figure 7A). The cells were cultured in vitro for 48 hours in erythroid differentiation medium. As we expected, the mDia2  $\Delta$ DAD mutant significantly induced overexpression of Chmp5 (supplemental Figure 7B) and rescued the defect in lysosome clearance and the increase in LC3B (supplemental Figure 7C-D) in mDia2-deficient erythroid cells. We next tested the role of Chmp5 in vivo in a transplantation model. To this end, the lineage-negative hematopoietic stem and progenitor cells from the bone marrow of mDia2<sup>fl/fl</sup>Vav-Cre mice were infected with retroviruses expressing Chmp5. The transduced cells that overexpressed Chmp5 were then transplanted into lethally irradiated wild-type recipient mice (Figure 7A). Compared with mice receiving vector-transduced mDia2-deficient bone marrow cells, those that received mDia2-deficient cells that overexpressed Chmp5 significantly rescued the RBC count and hemoglobin level 2 months after transplantation (Figure 7B; supplemental Figure 7E). Splenomegaly in mouse recipients of mDia2-deficient bone marrow diminished with the overexpression of Chmp5 (Figure 7C). When the bone marrow cells were harvested, we found that the binucleated orthochromatic erythroblasts that comprised almost half of the cells at this stage in



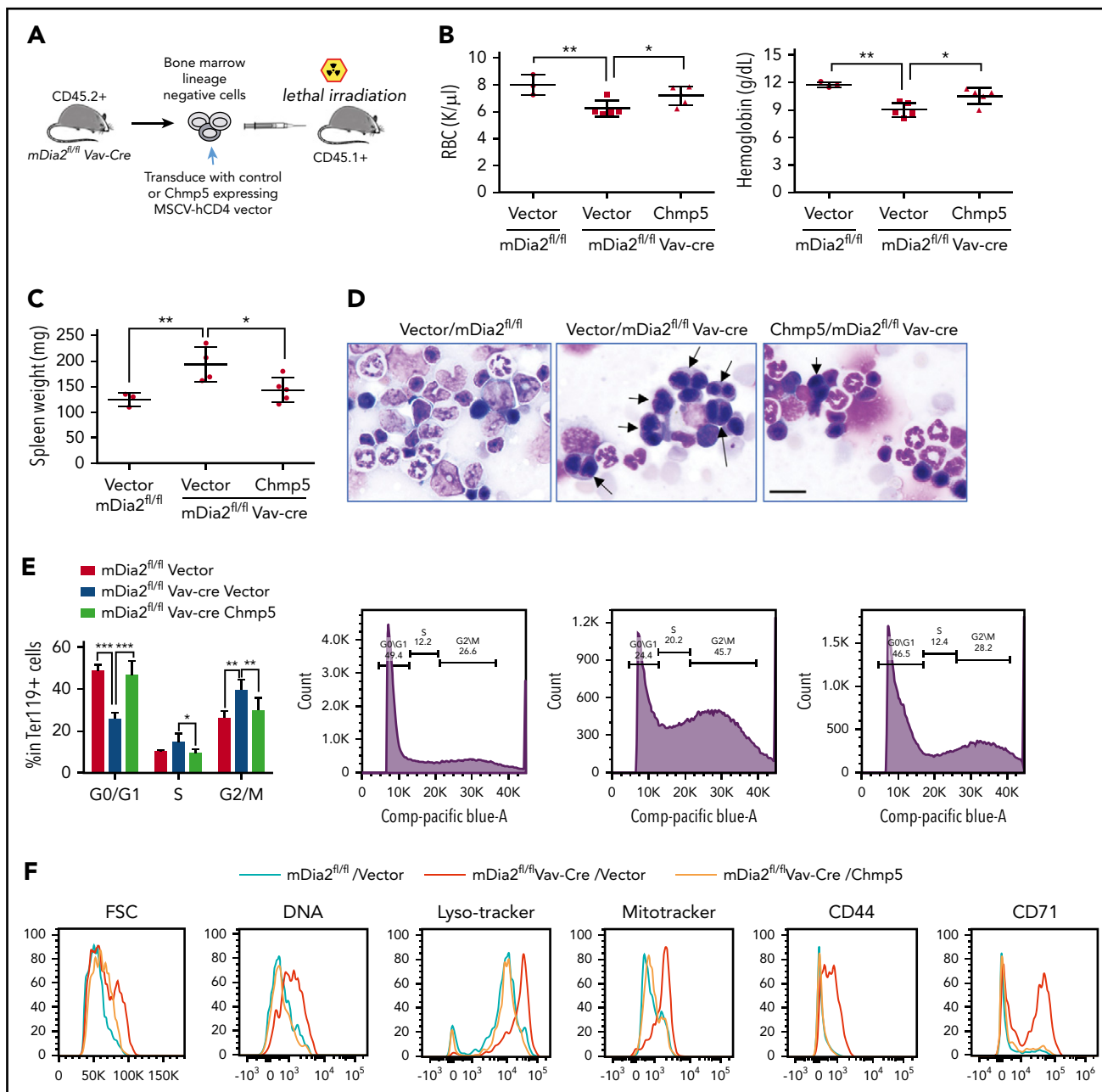


**Figure 7. Overexpression of Chmp5 ameliorates defects in late-stage terminal erythropoiesis in mDia2-deficient mice.** (A) Outline of the transplantation strategy. (B) RBC count and hemoglobin levels in mice receiving the indicated bone marrow cells for 2 months. (C) Spleen weight of mice in panel B. (D) Morphologic analyses of bone marrow smears from mice in panel B. Arrows indicate binucleated orthochromatic erythroblasts. Bar represents 20  $\mu$ m. Flow cytometric assays in the bottom panels quantify the percentage of S/G2/M phases reflecting the number of binucleated cells. (E) Quantitative analysis of panel D. (F) Lineage-negative cells from the bone marrow of the indicated recipient mice were cultured in erythropoietin-containing medium for 2 days. Flow cytometric analyses were performed with the indicated parameters to identify proteins on the reticulocytes. \* $P < .05$ ; \*\* $P < .01$ ; \*\*\* $P < .001$ .

mDia2-deficient mice were dramatically reduced with the overexpression of Chmp5 (Figure 7D-E). As expected, overexpression of Chmp5 also reversed the defects in organelle and protein clearance (Figure 7F), as well as the increase in autophagic flux (supplemental Figure 7F).

## Discussion

Our study revealed an important connection between the erythroid membrane actin skeleton and global proteome remodeling and organelle clearance during terminal erythropoiesis. The formin

protein mDia2 functions as a master regulator of this connection through polymerization of actin protofilaments, which signals the activation of SRF-mediated expression of different components of the ESCRT-III complex. Our results also demonstrated multiple functions of the ESCRT-III complex in the regulating endolysosomal and autolysosomal formation that are essential for membrane remodeling and cytoplasmic clearance during reticulocyte maturation. Furthermore, our results suggest that hereditary anemias that involve defects in membrane skeleton could also have compromised reticulocyte maturation. In addition, mDia formin proteins and the ESCRT-III complex could play broader

roles in mediating proteome remodeling and autophagy in other cell types.

One of the unsolved questions in erythroid membrane biology is how actin protofilaments are formed.<sup>58</sup> Our study revealed that mDia2 plays a critical role in this process. The disrupted actin protofilaments in mDia2-deficient reticulocytes led to reduced flexibility of the pseudo-hexagonal membrane skeleton meshwork, which explains the rigidity and lack of movement of the R1 reticulocytes during enucleation. Together with its role in contractile actin ring formation during enucleation,<sup>10,20</sup> mDia2 is essential for membrane integrity in the late stages of terminal erythropoiesis.

Notably, mDia2 plays multiple functions at different stages of terminal erythropoiesis. We and others have demonstrated that loss of mDia2 in fetal liver and adult bone marrow erythroid cells leads to cytokinesis defects before enucleation.<sup>19,20</sup> In this respect, we cannot completely exclude the possibility that the phenotypes we observed in mDia2-deficient reticulocytes are related to the absence of mDia2 in the early stages. However, that a brief Rac inhibitor treatment of the cultured erythroblasts immediately before enucleation caused a significant inhibition of enucleation suggests that nuclear detachment and reticulocyte motility are directly related to the specific function of mDia2 at this differentiation stage. Future studies using an mDia2 agonist or antagonist would be helpful in dissecting its specific roles in different stages of terminal erythropoiesis.

Our data demonstrate that erythroid cells are more sensitive to mDia2 deficiency but not its activation or overexpression. The sensitivity to mDia2 upregulation or downregulation appeared to be cell type specific. In HeLa cells, expression of a constitutively active mDia2 mutant leads to defects in cytokinesis.<sup>59</sup> In contrast, NIH 3T3 cells are more like erythroid cells and are sensitive to the loss of mDia2.<sup>60</sup> The sensitivity to mDia2 deficiency is also common in hematopoietic cells, in that loss of mDia2 can also lead to defects in the engraftment of hematopoietic stem and progenitor cells.<sup>22</sup>

Our results also revealed an important role of the membrane skeleton in protein sorting and endolysosome trafficking during reticulocyte maturation. Many surface proteins, such as CD71 and CD44, are programmed to be downregulated during the late stage of terminal erythropoiesis.<sup>36-38</sup> The possible mechanisms involve endocytosis, intracellular vesicle trafficking, and exocytosis.<sup>61,62</sup> During this process, surface proteins, as well as many other intracellular organelles and DNA-associated proteins, are removed through endosome-MVB-lysosome-autolysosome formation. Loss of mDia2 significantly compromises this process, which leads to the accumulation of large MVBs in orthochromatic erythroblasts and reticulocytes. More interesting, mDia2 deficiency also significantly affects the fusion of autophagosome and lysosome. The multifunctional properties of mDia2 prompted us to evaluate the ESCRT complexes that are involved in many of the similar processes. Indeed, many components of the ESCRT III complex were downregulated, including Chmp5.

As a formin protein, mDia2 not only functions in actin polymerization, but is also involved in transcriptional regulation through the MAL-SRF pathway.<sup>50</sup> The mDia2-SRF-Chmp5 pathway represents one of the first signaling cascades involved in the final stages of terminal erythropoiesis. This pathway regulates the cytokinesis of the last step of mitosis in orthochromatic erythroblasts, membrane and proteome remodeling, and endolysosome trafficking. Defects in all of these processes together contribute to lethal anemia during embryogenesis and ineffective erythropoiesis in adult mDia2-null mice, which also mimic certain inherited diseases in humans, such as congenital dyserythropoietic anemia.<sup>63</sup> Therefore, the results of our study could shed light on the pathogenesis of these human diseases.

## Acknowledgments

The authors thank the Robert H. Lurie Comprehensive Cancer Center flow cytometry core facility for help with the flow cytometry experiments and Congcong He for helpful discussions and for providing the lenti-mCherry-EGFP-LC3 construct and GFP-LC3 mice.

This work was supported by National Institutes of Health, National Institute of Diabetes and Digestive and Kidney Diseases (NIDDK) grant R01-DK124220 (P.J.), National Heart, Lung, and Blood Institute (NHBLI) grants R01-HL148012 and R01-HL150729 (P.J.) and R01-HL125710 (D.F.), National Cancer Institute Department of Defense grant CA140119 (P.J.), and National Institute of General Medical Sciences (NIGMS) grants GM132129 (J.A.P.) and GM97645 (S.P.G.). Z.P. was supported by National Science Foundation grant 1706436-CBET. P.J. is a scholar of the Leukemia and Lymphoma Society and the Harrington Discovery Institute.

## Authorship

Contribution: Y.L., Y.M., X.H., F.V.K., M.A.P., J.Y., and Z.P. performed the experiments and interpreted the data; J.A.P., S.P.G., and D.F. interpreted data; and Y.L. and P.J. designed the experiments, interpreted the data, and wrote and edited the manuscript.

Conflict-of-interest disclosure: The authors declare no competing financial interests.

ORCID profiles: J.A.P., 0000-0002-4291-413X; P.J., 0000-0002-8849-3625.

Correspondence: Peng Ji, Department of Pathology, Feinberg School of Medicine, Northwestern University, 303 East Chicago Ave, Ward 3-230, Chicago, IL 60611; e-mail: peng-ji@fsm.northwestern.edu.

## Footnotes

Submitted 27 April 2020; accepted 22 September 2020; prepublished online on *Blood* First Edition 9 October 2020. DOI 10.1182/blood.2020006673.

For original data, please e-mail the corresponding author.

The online version of this article contains a data supplement.

The publication costs of this article were defrayed in part by page charge payment. Therefore, and solely to indicate this fact, this article is hereby marked "advertisement" in accordance with 18 USC section 1734.

## REFERENCES

- Ovchinnikova E, Agliarolo F, von Lindern M, van den Akker E. The Shape Shifting Story of Reticulocyte Maturation. *Front Physiol.* 2018;9:829.
- Griffiths RE, Kupzic S, Cogan N, et al. Maturing reticulocytes internalize plasma membrane in glycophorin A-containing vesicles that fuse with autophagosomes before exocytosis. *Blood.* 2012;119(26):6296-6306.
- Johnstone RM, Adam M, Hammond JR, Orr L, Turbide C. Vesicle formation during reticulocyte maturation. Association of plasma membrane activities with released vesicles (exosomes). *J Biol Chem.* 1987;262(19):9412-9420.
- Mohandas N, Gallagher PG. Red cell membrane: past, present, and future. *Blood.* 2008;112(10):3939-3948.
- Woods CM, Lazarides E. The erythroid membrane skeleton: expression and assembly during erythropoiesis. *Annu Rev Med.* 1988;39(1):107-122.
- Chasis JA, Prenant M, Leung A, Mohandas N. Membrane assembly and remodeling during reticulocyte maturation. *Blood.* 1989;74(3):1112-1120.
- Liu J, Guo X, Mohandas N, Chasis JA, An X. Membrane remodeling during reticulocyte maturation. *Blood.* 2010;115(10):2021-2027.
- Liu J, Mohandas N, An X. Membrane assembly during erythropoiesis. *Curr Opin Hematol.* 2011;18(3):133-138.
- Lupo F, Tibaldi E, Matte A, et al. A new molecular link between defective autophagy and erythroid abnormalities in chorea-acanthocytosis. *Blood.* 2016;128(25):2976-2987.
- Ji P, Jayapal SR, Lodish HF. Enucleation of cultured mouse fetal erythroblasts requires Rac GTPases and mDia2. *Nat Cell Biol.* 2008;10(3):314-321.
- Faix J, Grosse R. Staying in shape with formins. *Dev Cell.* 2006;10(6):693-706.
- Kato T, Watanabe N, Morishima Y, Fujita A, Ishizaki T, Narumiya S. Localization of a mammalian homolog of diaphanous, mDia1, to the mitotic spindle in HeLa cells. *J Cell Sci.* 2001;114(Pt 4):775-784.
- Alberts AS. Identification of a carboxyl-terminal diaphanous-related formin homology protein autoregulatory domain. *J Biol Chem.* 2001;276(4):2824-2830.
- Palazzo AF, Cook TA, Alberts AS, Gundersen GG. mDia mediates Rho-regulated formation and orientation of stable microtubules. *Nat Cell Biol.* 2001;3(8):723-729.
- Schönichen A, Alexander M, Gasteier JE, Cuesta FE, Fackler OT, Geyer M. Biochemical characterization of the diaphanous autoregulatory interaction in the formin homology protein FHOD1. *J Biol Chem.* 2006;281(8):5084-5093.
- Tominaga T, Meng W, Togashi K, Urano H, Alberts AS, Tominaga M. The Rho GTPase effector protein, mDia, inhibits the DNA binding ability of the transcription factor Pax6 and changes the pattern of neurite extension in cerebellar granule cells through its binding to Pax6. *J Biol Chem.* 2002;277(49):47686-47691.
- Waller BJ, Stropich BN, Schoenherr JA, Holman HA, Kitchen SM, Alberts AS. The basic region of the diaphanous-autoregulatory domain (DAD) is required for autoregulatory interactions with the diaphanous-related formin inhibitory domain. *J Biol Chem.* 2006;281(7):4300-4307.
- Mao Y. FORMIN a link between kinetochores and microtubule ends. *Trends Cell Biol.* 2011;21(11):625-629.
- Watanabe S, De Zan T, Ishizaki T, et al. Loss of a Rho-regulated actin nucleator, mDia2, impairs cytokinesis during mouse fetal erythropoiesis. *Cell Rep.* 2013;5(4):926-932.
- Mei Y, Zhao B, Yang J, et al. Ineffective erythropoiesis caused by binucleated late-stage erythroblasts in mDia2 hematopoietic specific knockout mice. *Haematologica.* 2016;101(1):e1-e5.
- Keerthivasan G, Mei Y, Zhao B, et al. Aberrant overexpression of CD14 on granulocytes sensitizes the innate immune response in mDia1 heterozygous del(5q) MDS. *Blood.* 2014;124(5):780-790.
- Mei Y, Han X, Liu Y, Yang J, Sumagin R, Ji P. Diaphanous-related formin mDia2 regulates beta2 integrins to control hematopoietic stem and progenitor cell engraftment. *Nat Commun.* 2020;11(1):3172.
- Pan L, Yan R, Li W, Xu K. Super-Resolution Microscopy Reveals the Native Ultrastructure of the Erythrocyte Cytoskeleton. *Cell Rep.* 2018;22(5):1151-1158.
- Korobova F, Svitkina T. Molecular architecture of synaptic actin cytoskeleton in hippocampal neurons reveals a mechanism of dendritic spine morphogenesis. *Mol Biol Cell.* 2010;21(1):165-176.
- Stastna J, Pan X, Wang H, et al. Differing and isoform-specific roles for the formin DIAPH3 in plasma membrane blebbing and filopodia formation. *Cell Res.* 2012;22(4):728-745.
- Rana MK, Aloisio FM, Choi C, Barber DL. Formin-dependent TGF- $\beta$  signaling for epithelial to mesenchymal transition. *Mol Biol Cell.* 2018;29(12):1465-1475.
- Lu Y, Hanada T, Fujiwara Y, et al. Gene disruption of dematin causes precipitous loss of erythrocyte membrane stability and severe hemolytic anemia. *Blood.* 2016;128(1):93-103.
- Zhao B, Tan TL, Mei Y, et al. H2AX deficiency is associated with erythroid dysplasia and compromised haematopoietic stem cell function. *Sci Rep.* 2016;6(1):19589.
- Mei Y, Zhao B, Basiorka AA, et al. Age-related inflammatory bone marrow microenvironment induces ineffective erythropoiesis mimicking del(5q) MDS. *Leukemia.* 2018;32(4):1023-1033.
- Zhao B, Mei Y, Cao L, et al. Loss of pleckstrin-2 reverts lethality and vascular occlusions in JAK2V617F-positive myeloproliferative neoplasms. *J Clin Invest.* 2018;128(1):125-140.
- Zhao B, Mei Y, Schipma MJ, et al. Nuclear Condensation during Mouse Erythropoiesis Requires Caspase-3-Mediated Nuclear Opening. *Dev Cell.* 2016;36(5):498-510.
- Zhao B, Mei Y, Yang J, Ji P. Mouse fetal liver culture system to dissect target gene functions at the early and late stages of terminal erythropoiesis. *J Vis Exp.* 2014;(91):e51894.
- Zhao B, Keerthivasan G, Mei Y, et al. Targeted shRNA screening identified critical roles of pleckstrin-2 in erythropoiesis. *Haematologica.* 2014;99(7):1157-1167.
- Zhao B, Mei Y, Yang J, Ji P. Erythropoietin-regulated oxidative stress negatively affects enucleation during terminal erythropoiesis. *Exp Hematol.* 2016;44(10):975-981.
- Ji P, Murata-Hori M, Lodish HF. Formation of mammalian erythrocytes: chromatin condensation and enucleation. *Trends Cell Biol.* 2011;21(7):409-415.
- Tachiyama R, Ishikawa D, Matsumoto M, et al. Proteome of ubiquitin/MVB pathway: possible involvement of iron-induced ubiquitylation of transferrin receptor in lysosomal degradation. *Genes Cells.* 2011;16(4):448-466.
- Chen K, Liu J, Heck S, Chasis JA, An X, Mohandas N. Resolving the distinct stages in erythroid differentiation based on dynamic changes in membrane protein expression during erythropoiesis. *Proc Natl Acad Sci USA.* 2009;106(41):17413-17418.
- Liu J, Zhang J, Ginzburg Y, et al. Quantitative analysis of murine terminal erythroid differentiation in vivo: novel method to study normal and disordered erythropoiesis. *Blood.* 2013;121(8):e43-e49.
- Nguyen AT, Prado MA, Schmidt PJ, et al. UBE2O remodels the proteome during terminal erythroid differentiation. *Science.* 2017;357(6350):eaan0218.
- Simpson CF, Kling JM. The mechanism of denucleation in circulating erythroblasts. *J Cell Biol.* 1967;35(1):237-245.
- Babst M, Katzmann DJ, Estepa-Sabal EJ, Meerloo T, Emr SD. Escrt-III: an endosome-associated heterooligomeric protein complex required for mvb sorting. *Dev Cell.* 2002;3(2):271-282.
- Teis D, Saksena S, Emr SD. Ordered assembly of the ESCRT-III complex on endosomes is required to sequester cargo during MVB formation. *Dev Cell.* 2008;15(4):578-589.
- Shields SB, Oestreich AJ, Winistorfer S, et al. ESCRT ubiquitin-binding domains function cooperatively during MVB cargo sorting. *J Cell Biol.* 2009;185(2):213-224.
- Caballe A, Martin-Serrano J. ESCRT machinery and cytokinesis: the road to daughter cell separation. *Traffic.* 2011;12(10):1318-1326.
- Babst M. MVB vesicle formation: ESCRT-dependent, ESCRT-independent and everything in between. *Curr Opin Cell Biol.* 2011;23(4):452-457.
- Adell MA, Vogel GF, Pakdel M, et al. Coordinated binding of Vps4 to ESCRT-III drives membrane neck constriction during MVB vesicle formation. *J Cell Biol.* 2014;205(1):33-49.

47. Stoten CL, Carlton JG. ESCRT-dependent control of membrane remodelling during cell division. *Semin Cell Dev Biol.* 2018;74:50-65.
48. Shim JH, Xiao C, Hayden MS, et al. CHMP5 is essential for late endosome function and down-regulation of receptor signaling during mouse embryogenesis. *J Cell Biol.* 2006; 172(7):1045-1056.
49. Greenblatt MB, Park KH, Oh H, et al. CHMP5 controls bone turnover rates by dampening NF- $\kappa$ B activity in osteoclasts. *J Exp Med.* 2015; 212(8):1283-1301.
50. Baarlink C, Wang H, Grosse R. Nuclear actin network assembly by formins regulates the SRF coactivator MAL. *Science.* 2013; 340(6134):864-867.
51. Miralles F, Posern G, Zaromytidou AI, Treisman R. Actin dynamics control SRF activity by regulation of its coactivator MAL. *Cell.* 2003;113(3):329-342.
52. Eisenmann KM, Dykema KJ, Matheson SF, et al. 5q- myelodysplastic syndromes: chromosome 5q genes direct a tumor-suppression network sensing actin dynamics. *Oncogene.* 2009;28(39):3429-3441.
53. Poser S, Impey S, Trinh K, Xia Z, Storm DR. SRF-dependent gene expression is required for PI3-kinase-regulated cell proliferation. *EMBO J.* 2000;19(18): 4955-4966.
54. Tsunoda T, Takagi T. Estimating transcription factor bindability on DNA. *Bioinformatics.* 1999;15(7-8):622-630.
55. Takahashi Y, He H, Tang Z, et al. An autophagy assay reveals the ESCRT-III component CHMP2A as a regulator of phagophore closure. *Nat Commun.* 2018; 9(1):2855.
56. Klionsky DJ, Abdelmohsen K, Abe A, et al. Guidelines for the use and interpretation of assays for monitoring autophagy (3rd edition). *Autophagy.* 2016;12(1):1-222.
57. Mauthe M, Orhon I, Rocchi C, et al. Chloroquine inhibits autophagic flux by decreasing autophagosome-lysosome fusion. *Autophagy.* 2018;14(8):1435-1455.
58. Lux SE IV. Anatomy of the red cell membrane skeleton: unanswered questions. *Blood.* 2016; 127(2):187-199.
59. DeWard AD, Alberts AS. Ubiquitin-mediated degradation of the formin mDia2 upon completion of cell division. *J Biol Chem.* 2009; 284(30):20061-20069.
60. Watanabe S, Ando Y, Yasuda S, et al. mDia2 induces the actin scaffold for the contractile ring and stabilizes its position during cytokinesis in NIH 3T3 cells. *Mol Biol Cell.* 2008; 19(5):2328-2338.
61. Keerthivasan G, Small S, Liu H, Wickrema A, Crispino JD. Vesicle trafficking plays a novel role in erythroblast enucleation. *Blood.* 2010; 116(17):3331-3340.
62. Blanc L, Liu J, Vidal M, Chasis JA, An X, Mohandas N. The water channel aquaporin-1 partitions into exosomes during reticulocyte maturation: implication for the regulation of cell volume. *Blood.* 2009;114(18): 3928-3934.
63. Resnitzky P, Shaft D, Shalev H, et al. Morphological features of congenital dyserythropoietic anemia type I: The role of electron microscopy in diagnosis. *Eur J Haematol.* 2017;99(4): 366-371.